Environmental Science & Technology

Article

pubs.acs.org/est

# Predicting Reduction Rates of Energetic Nitroaromatic Compounds Using Calculated One-Electron Reduction Potentials

Alexandra J. Salter-Blanc,[†] Eric J. Bylaska,[‡] Hayley J. Johnston,[†] and Paul G. Tratnyek*[,†]

[†]Institute of Environmental Health, Oregon Health & Science University, 3181 SW Sam Jackson Park Road, Portland, Oregon 97239-3098, United States

[‡]William R. Wiley Environmental Molecular Sciences Laboratory, Pacific Northwest National Laboratory, P.O. Box 999, Richland, Washington 99352, United States

Supporting Information

**ABSTRACT:** The evaluation of new energetic nitroaromatic compounds (NACs) for use in green munitions formulations requires models that can predict their environmental fate. Previously invoked linear free energy relationships (LFER) relating the log of the rate constant for this reaction (log($k$)) and one-electron reduction potentials for the NAC ($E^1_{NAC}$) normalized to 0.059 V have been re-evaluated and compared to a new analysis using a (nonlinear) free-energy relationship (FER) based on the Marcus theory of outer-sphere electron transfer. For most reductants, the results are inconsistent with simple rate limitation by an initial, outer-sphere electron transfer, suggesting that the linear correlation between log($k$) and $E^1_{NAC}$ is best regarded as an empirical model. This correlation was used to calibrate a new quantitative structure−activity relationship (QSAR) using previously reported values of log($k$) for nonenergetic NAC reduction by Fe(II) porphyrin and newly reported values of $E^1_{NAC}$ determined using density functional theory at the M06-2X/6-311++G(2d,2p) level with the COSMO solvation model. The QSAR was then validated for energetic NACs using newly measured kinetic data for 2,4,6-trinitrotoluene (TNT), 2,4-dinitrotoluene (2,4-DNT), and 2,4-dinitroanisole (DNAN). The data show close agreement with the QSAR, supporting its applicability to other energetic NACs.

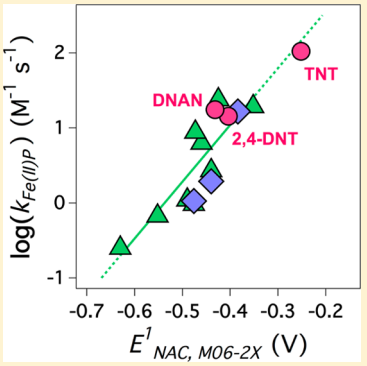


## INTRODUCTION

The release of energetic nitroaromatic compounds (NACs) used in munitions (e.g., during manufacturing and in application for testing and training), poses known and potential threats to human health and the environment.[1,2] Concern over these risks has led to interest in identifying new energetic compounds with properties that minimize their environmental impact.[3] This application of green chemistry principals[4] to the design and selection of new energetic compounds requires data on their chemical fate properties, often in the early stages of evaluation (including prior to synthesis) when experimentation with the candidate compounds is impractical.[3,5] To overcome this obstacle, robust models are needed to predict key environmental fate properties, including rate constants for nitro reduction, which is a major determinant of their fate.[6,7]

In a substantial amount of previous work,[(e.g., 6,8−10)] linear correlations of NAC reduction rate constants in the presence of a variety of reductants ($k_{red}$) were related to one-electron reduction potentials ($E^1_{NAC}$) according to the following linear free energy relationship (LFER) (eq 1).

$$\log k_{red} = a\frac{E^1_{NAC}}{2.3RT/F} + b = a\frac{E^1_{NAC}}{0.059\ \mathrm{V}} + b \quad (1)$$

Many of the correlations reported using eq 1 have a slope ($a$) of ∼1 and this has widely been interpreted as evidence that the rate-limiting step in NAC reduction is the initial electron transfer in an outer-sphere reaction (eq 2).[6]

$$Ar{-}NO_2 + e^- \rightleftharpoons Ar{-}NO_2^{\bullet -} \quad (2)$$

Electrochemical studies of NAC reduction, however, suggest that subsequent reaction steps—either dehydration or electron transfer to Ar−$NO_2^{\bullet -}$—are rate limiting, depending on experimental conditions.[11,12] In addition, evidence from compound-specific nitrogen isotope analysis of NAC reduction reactions suggests that the rate limiting step in NAC reduction is either (i) the dehydration of Ar−$N(OH)_2$ to form Ar−NO, or (ii) proton or electron transfer to the nitroaromatic radical anion (Ar−$NO_2^{\bullet -}$), depending on the reductant and solution chemistry.[13−15] In the latter work, it was suggested that the initial electron transfer might still influence the overall rate of NAC reduction if it served as a pre-equilibrium step before subsequent slower steps.[13]

To provide additional reconciliation between the common interpretation of LFERs involving NAC reduction and the apparent inconsistency with evidence from electrochemical and isotope fractionation studies—and to provide a more

Received: October 20, 2014
Revised: February 5, 2015
Accepted: February 11, 2015
Published: February 11, 2015

  

DOI: 10.1021/es505092s
Environ. Sci. Technol. 2015, 49, 3778−3786

thoroughly vetted basis for defining predictive models for energetic NAC compounds—we have revisited the interpretation of the correlation between $\log(k_{red})$ and $E^1_{NAC}$ as evidence that initial outer-sphere electron transfer is rate limiting. This was done by comparing the LFER described in eq 1 and a (nonlinear) free energy relationship (FER) based on the Marcus theory of outer-sphere electron transfer,[16] developed for application to organic reactions by Eberson.[17] The Marcus–Eberson approach (described in detail in the Background section) has been used to analyze kinetic data for a variety of organic reactions,[(e.g., 17,18)] including environmentally relevant oxidation reactions[19−21] and photocatalytic reduction of NACs by $TiO_2$.[22] However, somewhat surprisingly, this model has not previously been fully and quantitatively evaluated for describing the kinetics of NAC reduction by environmentally relevant model reductants. Therefore, the first major objective of this study was to reevaluate the application of (L)FERs for describing rates of NAC reduction by applying the Marcus–Eberson model to existing data for the reduction of NACs (by quinone and iron porphyrin electron shuttles and organically complexed Fe(II) species) and to assess the consistency of the results with evidence regarding the rate-limiting step of nitro reduction.

Our second and ultimate objective was to define a predictive correlation for nitro reduction by calibrating a (L)FER or quantitative structure−activity relationship (QSAR) with available kinetic data for nonenergetic model NACs and then testing its range of applicability using new data for available energetic NACs. Development of such a predictive model (and its future application) requires data for $E^1_{NAC}$, however, measured data for $E^1_{NAC}$ are often lacking or difficult to obtain, particularly for novel energetic NACs (e.g., due to lack of synthesized material or experimental hazards). To overcome this, it is desirable to use calculated values, such as those obtained using molecular modeling. Multiple efforts have been made to determine $E^1_{NAC}$ using various computational techniques.[23−28] We compiled and compared the results of many of these studies previously, in addition to presenting preliminary results from our own calculations of $E^1_{NAC}$.[26] In this paper, we have expanded on our previous results and applied these computational methods to a larger set of compounds. We also present kinetic data for the nitro reduction of three energetic NACs—2,4,6-trinitrotoluene (TNT), 2,4-dinitrotoluene (2,4-DNT), and 2,4-dinitroanisole (DNAN)—and use these to test the range of applicability of the correlation calibrated with nonenergetic model compounds.

## BACKGROUND

The Marcus theory of outer-sphere electron transfer relates the free energy of activation ($\Delta G^{\ddagger}$) for an electron transfer to the corrected standard free energy of the reaction ($\Delta G^{\circ\prime}$)[17,29] as shown in the following parabolic relationship:

$$\Delta G^{\ddagger} = W + \frac{\lambda}{4}\left(1 + \frac{\Delta G^{\circ\prime}}{\lambda}\right)^2 \tag{3}$$

where $W$ is an electrostatic term and $\lambda$ is the reorganization energy.[17] Based on the collide-and-react model of electron transfer (as described by Eberson[17]) the following equation has been derived to describe the observed reaction rate ($k$)

$$k = \frac{k_d}{1 + \frac{k_d}{K_d Z}\exp\left\{\left[W + \frac{\lambda}{4}\left(1 + \frac{\Delta G^{\circ\prime}}{\lambda}\right)^2\right]/RT\right\}} \tag{4}$$

where $k_d$ is the rate at which the electron donor and acceptor diffuse together to form the precursor complex, $K_d$ is the equilibrium constant for formation of the precursor complex, $Z$ is a universal frequency factor (describing collision frequency), and $R$ and $T$ have their usual meanings. Equation 4 accounts for contributions to $k$ from precursor formation (controlled by $k_d$) (i.e., diffusion together of the electron donor and acceptor compounds) and the rate of electron transfer ($k_{ET}$) from the electron donor to the acceptor.[17]

For the analysis presented in this work, values for the variables in eq 4 were defined or calculated as follows. $k_d$ and $k_d/K_dZ$ were assumed to be $10^{10}$ $M^{-1}$ $s^{-1}$ and 0.1, respectively—both common assumptions for these parameters, which have little influence on eq 4.[17] The value of $W$ depends on the charges on the electron acceptor and donor species ($Z_1$ and $Z_2$),[17] and is equal to zero when $Z_1$ and/or $Z_2$ = 0, as is the case in all instances presented here (because the charge on the NAC = 0 in all cases). Including these assumptions, a log transformation of eq 4 gives eq 5.

$$\log k = \log(10^{10}) - \log\left(1 + 0.1 \times \exp\left\{\left[\frac{\lambda}{4}\left(1 + \frac{\Delta G^{\circ}}{\lambda}\right)^2\right] /0.592\right\}\right) \tag{5}$$

Plots of eq 5 (i.e., "Marcus plots"[17]) are shown in Figure 1 for various $\lambda$. Nonlinear regression of eq 5 (where $\lambda$ is the only fitting parameter) to data for $\log(k)$ and $\Delta G^{\circ\prime}$ is one way to evaluate the consistency of a data set with the model assumption that the observed rate is controlled by outer-sphere electron transfer.[17]

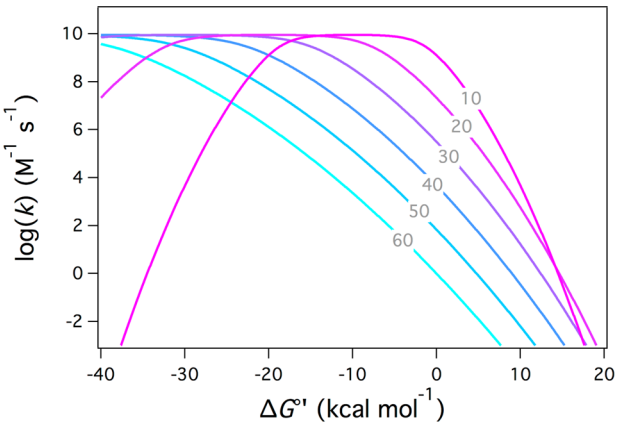


**Figure 1.** Generic Marcus plot of eq 5 for various values of $\lambda$ (labeled on the curves in kcal $mol^{-1}$). Other model assumptions are given in the text.

## EXPERIMENTAL SECTION

**Reagents.** Stock solutions of nitrobenzene (NB) (Aldrich Chemical Co. Inc.), 2,4,6-trinitrotoluene (TNT) (Chem Service Inc.), 1-chloro-4-nitrobenzene (4-Cl-NB) (Acros Organics), 2,4-dintroanisole (DNAN) (Alfa Aesar), 2,4-


DOI: 10.1021/es505092s
Environ. Sci. Technol. 2015, 49, 3778−3786

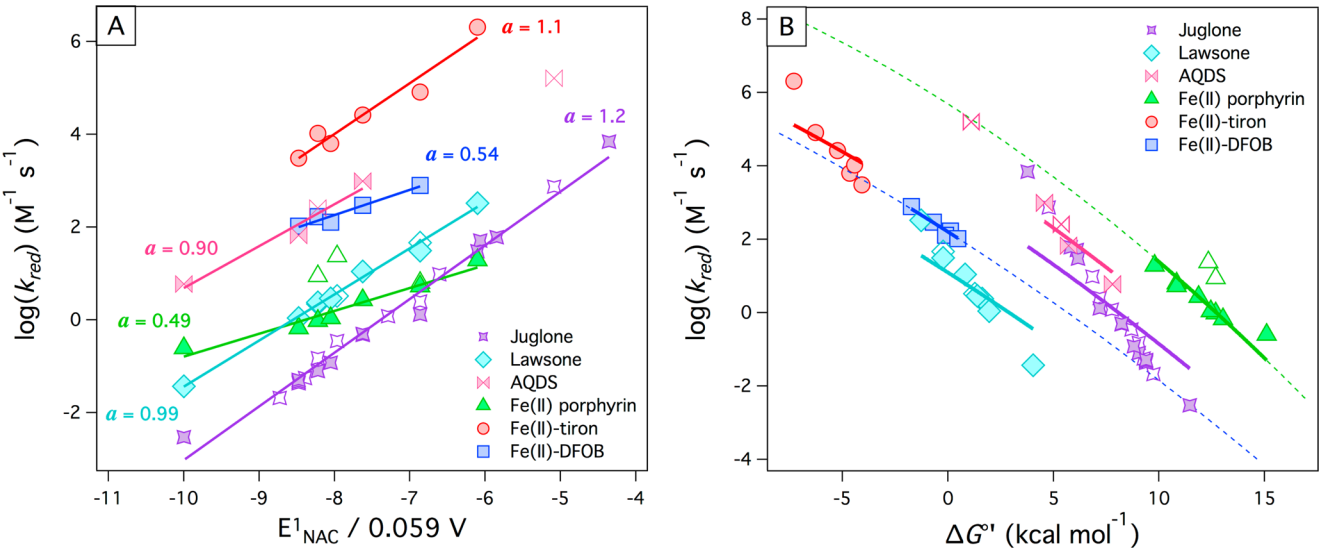


**Figure 2.** log($k_{red}$) for various NACs vs (A) $E^1_{NAC}$/0.059 V and (B) $\Delta G^{\circ\prime}$. Reductants include the electron carrier/donor pairs juglone/hydrogen sulfide,[8,9] lawsone/hydrogen sulfide,[8] Fe(II) porphyrin/cysteine,[8] electrochemically reduced AQDS,[14] and the Fe(II)−ligand complexes Fe(II)−tiron[41] and Fe(II)−DFOB.[42] Closed symbols represent data for which the descriptor variable was determined from measured $E^1_{red}$. Open symbols represent data for which the descriptor variable was determined from reported $E^1_{red}$ values that were estimated from LFERs.[8,9] Only data for which $E^1_{red}$ was measured were included in the fits. The data were fit to (A) eq 1 or (B) eq 5. In (B), an extrapolation of the fit is shown (as a dashed line) for cases where the data is well fit to eq 5.

dinitrotoluene (2,4-DNT) (Tokyo Chemical Industry Co.), and 1,3-dinitrobenzene (1,3-DNB) (Tokyo Chemical Industry Co.) were prepared in HPLC-grade methanol (Fisher Scientific) at a concentration of 0.1 M. Phosphate buffer was prepared from monobasic sodium phosphate (Fisher Scientific) and adjusted with NaOH (Aldrich) to pH 7.0. L-cysteine (Acros Organics) solutions (0.25 M) were prepared fresh daily in deoxygenated DI water. Stock solutions of Fe(III) meso-tetra (*N*-methyl-4-pyridyl) porphine pentachloride (Frontier Scientific) were prepared in deoxygenated DI water at a concentration of 4.29 mM. All deionized (DI) water used was obtained from a Milli-Q system (EMD Millipore).

**Batch Experiments.** Batch experiments were performed in 60-mL clear glass reaction vials capped with butyl rubber septa (Fisher Scientific). Each vial was prepared in an anoxic glovebox (5% $H_2$ in $N_2$) and initially contained 49 mL of 50 mM phosphate buffer, 1 mL of aqueous cysteine solution, and an aliquot (25−400 $\mu$L) of aqueous porphyrin stock solution. Vials were equilibrated to 25.0 °C in a water bath. After temperature equilibration, the specified NAC was introduced to the reaction vial by injecting 50 $\mu$L of a 0.1 M stock solution. One-mL aliquots were removed over time and quenched by mixing with an equal volume of oxygen-containing (i.e., not deoxygenated) HPLC grade methanol. Quenched aliquots were analyzed by high-performance liquid chromatography (HPLC) using a Varian ProStar 210 solvent delivery module, 410 autosampler, and 330 photodiode array detector, with a Platinum C18 5 $\mu$m 250 mm × 4.6 mm column (Grace). For most analyses, the mobile phase consisted of 1:1 DI water and HPLC-grade methanol, the flow rate was 1 mL $min^{-1}$, and the detection wavelength was 254 nm.

**Computational Methods.** The computational methods used in this study are fully described in the Supporting Information (SI), Section 1. Briefly, values of $E^1_{NAC}$ were determined from the free energy difference, $\Delta G_{rxn}$, for the one-electron half reaction, given in eq 2. These energy differences were calculated using electronic structure calculations with the COSMO[30] and COSMO-SMD continuum solvation models using the NWChem program suite.[31] The electronic structure calculations were performed using density functional theory (DFT)[32] with the 6-311++G(2d,2p) basis set[33,34] and the LDA,[35] PBE96,[36] B3LYP,[37,38] PBE0,[39] and M06-2X[40] exchange correlation functionals.

## RESULTS AND DISCUSSION

**Assessment of Free-Energy Relationships (FER).** To reevaluate the use of FERs to describe NAC reduction rates, and to assess the consistency of these FERs with other evidence regarding the rate-limiting step of this reaction, we compiled the major data sets for NAC reduction by homogeneous reductants (consisting of second order rate constants, $k_{red}$) and plotted the data vs $E^1_{NAC}$/0.059 V according to eq 1 (in the convention of previous studies)[(e.g., 6,8−10)] and vs $\Delta G^{\circ\prime}$ (in a Marcus plot). The results are shown in Figure 2A and B, respectively. The compiled data include $k_{red}$ for NAC reduction by the electron carrier/donor pairs juglone/hydrogen sulfide,[8,9] lawsone/hydrogen sulfide,[8] and Fe(II) porphyrin/cysteine,[8] as well as electrochemically reduced 9,10-anthraquinone-2,6-disolfonate (AQDS) and Fe(II) complexed by the organic ligands tiron[41] and desferrioxamine B (DFOB).[42] Throughout this paper, we refer to these redox systems simply as juglone, lawsone, AQDS, Fe(II) porphyrin, Fe(II)−tiron, and Fe(II)−DFOB.

The $E^1_{NAC}$ data used in the preparation of Figure 2 were those reported in conjunction with the original $k_{red}$ data sets.[8,9,41,42] Note that in some cases, the values of $E^1_{NAC}$ were not measured, but instead were estimated based on LFERs for juglone and lawsone.[9,10] We included these data in Figure 2 but excluded them from subsequent fitting. For Figure 2B, $\Delta G^{\circ\prime}$ was calculated for all NAC/reductant pairs. For this, it was determined that the electrostatic term differentiating $\Delta G^{\circ\prime}$ from $\Delta G^{\circ}$ (described in detail elsewhere)[17,29,43] was equal to zero in cases where the reductant carries a charge of −1,[17] and negligible in all other cases.[29,43] Therefore, $\Delta G^{\circ\prime}$ was taken to


DOI: 10.1021/es505092s
Environ. Sci. Technol. 2015, 49, 3778−3786

be equal to $\Delta G^\circ$. $\Delta G^\circ$ was calculated from $E^1_{NAC}$ and the one-electron reduction potential for the reductant ($E^1_{red}$) according to eq 6.

$$\Delta G^\circ = -nF[E^1_{NAC} - E^1_{red}] \quad (6)$$

where $n$ is the number of electrons transferred (assumed to be 1 in all cases), and $F$ is the Faraday constant. Care was taken to use $E^1$ values applicable to the experimental conditions. For example, because of the pH dependence of $E^1_{red}$, we used either potentials measured at pH 7 ($E^1_7$) or potentials corrected for standard environmental conditions ($E^{1\prime}$)[8] (both obtained from the literature[8,44,45]) when appropriate. When the experimental pH deviated from 7, $E^1_{red}$ was calculated from the standard one-electron reduction potentials ($E^0$).[41,42,46] Details on the sources of and corrections to $E^1$ are described in the SI, Tables S1−S6.

The data in Figure 2A (which in most cases are replots of previously reported correlations[8,9,47]) show strong linear correlations to $E^1_{NAC}$. When fit to eq 1, the following results are obtained: for juglone, $a = 1.2 \pm 0.052$; for lawsone, $a = 0.99 \pm 0.037$; for AQDS, $a = 0.90 \pm 0.18$; for Fe(II) porphyrin, $a = 0.05 \pm 0.48$; for Fe(II)−tiron, $a = 1.1 \pm 0.12$; and for Fe(II)−DFOB, $a = 0.54 \pm 0.07$. Slopes of this type have been interpreted mechanistically, as follows: "If in a given case, a significant correlation is found between $[\log(k_{red})]$ and $[E^1_{NAC}/0.059\ V]$ with a slope of close to 1.0, it can be concluded that, for the series of NACs (or any other compound class) considered, the actual transfer of the electron from the reductant to the compounds is rate determining. If a much weaker dependency of $[\log(k_{red})]$ on $[E^1_{NAC}]$ (i.e., a slope of a $\ll 1$), or no correlation at all is found, then other reaction steps and/or processes are important including, for example, precursor complex formation, the (slow) regeneration of reactive sites, and/or just plain mass transport."[6] This interpretation has been applied to the reduction of NACs by juglone, lawsone, and Fe(II) porphyrin (Fe(II)P) previously,[6,8,9] and extending the interpretation to the whole set of correlations shown in Figure 2A implies that while rates of NAC reduction by juglone, lawsone, AQDS, and Fe(II)−tiron may be limited by $k_{ET}$ (for the first electron transfer), the rates of NAC reduction by Fe(II) porphyrin (Fe(II)P) and Fe(II)/DFOB are influenced by other factors. However, these conclusions regarding the mechanism of NAC reduction are not entirely consistent with the results from electrochemical experiments and stable isotope analysis of NAC reduction by reductants including juglone, AQDS, and Fe(II)−tiron, which suggest later reaction steps are (primarily) rate limiting.[11−15]

To further evaluate the consistency of the kinetic data with a rate-controlling, initial electron transfer step, the $\log(k_{red})$ data shown in Figure 2A were plotted vs $\Delta G^{\circ\prime}$ and fit to the Marcus−Eberson model by using eq 5 (as shown in Figure 2B). Visual inspection of the data in Figure 2B shows fairly strong (ostensibly linear) correlations between $\log(k_{red})$ and $\Delta G^{\circ\prime}$ for each reductant. However, the correlations that are evident in Figure 2B do not always coincide with the fits to eq 5. For two of the reductants—Fe(II) porphyin and Fe(II)−DFOB—the correlations coincide well with fits to the Marcus−Eberson model: the data are fit closely and there are few outliers (one for Fe(II) porphyrin (solid green triangles) and none for Fe(II)−DFOB (solid blue squares)). These fits are shown in Figure 2B as solid curves with extrapolations shown in dashed lines. For the other reductants—juglone, lawsone, AQDS, and Fe(II)−tiron—the trends in the data cannot be matched by regression to eq 5, which is tightly constrained by having only one fitted variable ($\lambda$). We have included the curves that result from fitting these data in Figure 2B to show that the model consistently gives shallower "slopes" than the observed correlation.

The ability of the Marcus−Eberson model to fit the data for Fe(II) porphyin and Fe(II)−DFOB but not juglone, lawsone, AQDS, and Fe(II)−tiron is prima facie evidence that the former group conforms the assumptions of the model and the latter group does not. The deviation from the Marcus−Eberson model by the second group of reductants might be explained by a number of scenarios in which an initial, outer-sphere electron transfer is not primarily rate limiting—including scenarios of complex rate-limitation in which later reaction steps influence the observed rate, as suggested by evidence from compound-specific isotope analysis of NAC reduction by juglone, AQDS, and Fe(II)−tiron.[13−15]

The conclusions we have drawn from Figure 2B regarding consistency of the kinetic data with Marcus theory differ from the interpretations others have drawn previously based on correlations to $E^1_{NAC}$ fit to eq 1 (Figure 2A). Specifically, the reductants that produce a slope of ∼1 in Figure 2A (previously interpreted as indicative of rate control by $k_{ET}$ within the first electron transfer step) are the same reductants where the trend in the data is not adequately captured by fitting to eq 5 in Figure 2B, suggesting the rate is not primarily controlled by the overall rate of an initial, outer-sphere electron transfer (influenced by both $k_{ET}$ and $k_d$). Also, the reductants that produce a slope of $\ll 1$ in Figure 2A (previously interpreted as indicative of rate control by factors other than the first electron transfer) are well-fit by eq 5, suggesting that these reductants react in a manner more consistent with the Marcus−Eberson model. The reason for this inverse interpretation of the two figures is explored below.

Equation 1 is similar to the Marcus−Eberson FER (eq 4), but with two major simplifications: (i) eq 1 is based on a linear model by Polanyi rather than the quadratic model by Marcus,[6,10,48,49] and (ii) it has been rewritten in terms of $E^1_{NAC,}$[10] rather than $\Delta G^{\circ\prime}$. Over sufficiently small ranges of $\Delta G^{\circ\prime}$, the Polanyi equation describes the tangent to the curve described by the Marcus equation. Tangents to the Marcus curve have been classified into three regions: (i) an inverted region where the tangent has a slope ($\gamma$) > 0 (not relevant here); (ii) a plateau region where $k_d$ is controlling (i.e., precursor formation is rate limiting) and $\gamma = 0$; and (iii) a curved region where electron transfer is rate limiting and $\gamma < 0$.[17,29] It should be noted that this interpretation assumes irreversible electron transfer (on the basis that the rate of reverse electron transfer is insignificant).[17] If $k_{ET}$ is relatively slow, then an additional term can be added to eq 4 to account for reverse electron transfer and competition of this reaction step with the formation of successor complexes (as described elsewhere[17,29,50]). In this case, the slope of region iii approaches a limiting value of $\gamma = -1/2.3RT$ at sufficiently endergonic reactions.[17,29,50] In either case, the slopes of these tangents can be reliably interpreted as consistent or inconsistent with Marcus theory (without performing nonlinear regression) only if the relationship between the tangent and $\Delta G^{\circ\prime}$ is taken into account (i.e., the tangent should have $\gamma = -0.5/2.3RT$ only at $\Delta G^{\circ\prime} = 0$, $\gamma < -0.5/2.3RT$ only at $\Delta G^{\circ\prime} > 0$, and $\gamma > -0.5/2.3RT$ only at $\Delta G^{\circ\prime} < 0$).[29] Because eq 1 is written in terms of $E^1_{NAC}$ (with $E^1_{red}$ factored into the constant $b$),[10] the relationship between the descriptor data and $\Delta G^{\circ\prime}$ is obscured and the influence of $E^1_{red}$ is neglected.



DOI: 10.1021/es505092s
Environ. Sci. Technol. 2015, 49, 3778−3786

Table 1. Calculated One-Electron Reduction Potentials ($E^1_{NAC}$) and Comparison to a Set of Measured Values[a]

| | | calculated $E^1_{NAC}$ (V) | | | | | | |
|---|---|---|---|---|---|---|---|---|
| | | COSMO | | | | | COSMO-SMD | |
| abbreviation[b] | measured $E^1_{NAC}$ (V)[c] | LDA | PBE | PBE0 | B3LYP | M06-2X | B3LYP | M06-2X |
| NB | −0.486 | −0.512 | −0.640 | −0.578 | −0.479 | −0.476 | −0.402 | −0.404 |
| 2-$CH_3$-NB | −0.590 | −0.659 | −0.771 | −0.695 | −0.616 | −0.630 | −0.548 | −0.619 |
| 3-$CH_3$-NB | −0.475 | −0.561 | −0.690 | −0.602 | −0.522 | −0.490 | −0.444 | −0.438 |
| 4-$CH_3$-NB | −0.500 | −0.594 | −0.726 | −0.637 | −0.569 | −0.552 | −0.469 | −0.465 |
| 3-Cl-NB | −0.405 | −0.272 | −0.545 | −0.487 | −0.400 | −0.571 | −0.341 | −0.350 |
| 4-Cl-NB | −0.450 | −0.475 | −0.599 | −0.539 | −0.444 | −0.440 | −0.382 | −0.388 |
| 4-$NH_2$-NB | −0.568 | −0.964 | −1.043 | −0.863 | −0.753 | −0.737 | −0.669 | −0.776 |
| 3-$COCH_3$-NB | −0.437 | −0.439 | −0.586 | −0.538 | −0.469 | −0.460 | −0.385 | −0.376 |
| 4-$COCH_3$-NB | −0.356 | −0.174 | −0.354 | −0.375 | −0.304 | −0.352 | −0.222 | −0.261 |
| 1,2-DNB | −0.287 | 0.033 | −0.169 | −0.230 | −0.121 | −0.299 | −0.016 | −0.157 |
| 1,3-DNB | −0.345 | −0.339 | −0.581 | −0.505 | −0.390 | −0.384 | −0.165 | −0.243 |
| 1,4-DNB | −0.257 | 0.197 | 0.011 | −0.075 | 0.059 | −0.117 | 0.131 | −0.052 |
| 2,4-DNT | −0.397 | −0.542 | −0.638 | −0.618 | −0.486 | −0.404 | −0.441 | −0.317 |
| 2,6-DNT | −0.402 | −0.318 | −0.718 | −0.682 | −0.569 | −0.525 | −0.513 | −0.407 |
| TNT | −0.253 | −0.232 | −0.384 | −0.378 | −0.223 | −0.252 | −0.191 | −0.153 |
| 2-CHO | −0.355 | −0.151 | −0.345 | −0.361 | −0.271 | −0.341 | −0.225 | −0.272 |
| 4-CHO | −0.322 | −0.065 | −0.255 | −0.273 | −0.216 | −0.364 | −0.126 | −0.229 |
| 4-$CH_2OH$ | −0.478 | −0.554 | −0.642 | −0.624 | −0.501 | −0.561 | −0.419 | −0.458 |
| 2-ADNT | −0.417 | −0.586 | −0.729 | −0.642 | −0.554 | −0.466 | −0.480 | −0.384 |
| 4-ADNT | −0.449 | −0.707 | −0.753 | −0.700 | −0.629 | −0.571 | −0.523 | −0.467 |
| 2,4-DANT | −0.502 | −0.870 | −0.995 | −0.876 | −0.810 | −0.775 | −0.697 | −0.465 |
| 2-Cl-NB | | −0.458 | −0.599 | −0.533 | −0.462 | −0.473 | −0.433 | −0.461 |
| 2-$COCH_3$-NB | | −0.424 | −0.588 | −0.600 | −0.425 | −0.425 | −0.396 | −0.434 |
| DNAN | | −0.517 | −0.827 | −0.652 | −0.463 | −0.432 | −0.482 | −0.371 |
| MAD[d] | | 0.161 | 0.207 | 0.149 | 0.099 | 0.066 | 0.113 | 0.075 |
| RMSD[e] | | 0.043 | 0.058 | 0.031 | 0.018 | 0.009 | 0.021 | 0.008 |
| largest positive deviation | | 0.454[f] | 0.268[f] | 0.182[f] | 0.316[f] | 0.140[f] | 0.388[f] | 0.205[f] |
| largest negative deviation | | −0.396[g] | −0.493[h] | −0.374[h] | −0.308[h] | −0.273[h] | −0.195[h] | −0.208[g] |

[a]Calculated values were determined with density functional theory (DFT) using the 6-311++G(2d,2p) basis set with the specified exchange correlation functionals and solvation models. [b]Abbreviations: nitrobenzene (NB), 2-methylnitrobenzene (2-$CH_3$-NB), 3-methylnitrobenzene (3-$CH_3$-NB), 4-methylnitrobenzene (4-$CH_3$-NB), 3-chloronitrobenzene (3-Cl-NB), 4-chloronitrobenzene (4-Cl-NB), 4-nitroaniline (4-$NH_2$-NB), 3-acetylnitrobenzene (3-$COCH_3$-NB), 4-acetylnitrobenzene (4-$COCH_3$-NB), 1,2-dinitrobenzene (1,2-DNB), 1,3-dinitrobenzene (1,3-DNB), 1,4-dinitrobenzene (1,4-DNB), 2,4-dinitrotoluene (2,4-DNT), 2,6-dinitrotoluene (2,6-DNT), 2,4,6-trinitrotoluene (TNT), 2-nitrobenzaldehyde (2-CHO), 4-nitrobenzaldehyde (4-CHO), 4-nitrobenzyl alcohol (4-$CH_2OH$), 2-amino-4,6-dinitrotoluene (2-ADNT), 4-amino-2,5-dinitrotoluene (4-ADNT), 2,4-diamino-6-nitrotoluene (2,4-DANT). [c]Data set previously compiled by Phillips et al.[51] [d]Mean absolute deviation. [e]Root mean square deviation. [f]Deviant value for 1,4-DNB. [g]Deviant value for 4-$NH_2$−NB. [h]Deviant value for 2,4-DANT.

To further demonstrate the risk of neglecting $E^1_{red}$, the data in Figure 2B were fit to a version of eq 5 that was written in terms of $E^1_{NAC}$ (by substituting in eq 6 for $\Delta G^{\circ\prime}$), thereby allowing both $\lambda$ and $E^1_{red}$ to be fitting parameters. Adding this additional degree of freedom to the fitting equation produced fits (not shown) that agree closely with the trends for all of the reductants, including juglone, lawsone, and Fe(II)/tiron. However, some of the fitted values for $E^1_{red}$ were implausibly different from the measured values (e.g., for lawsone, the fitted value of $E^1_{red}$ was 0.144 V, whereas the measured value is −0.415 V[45] and for juglone, the fitted value of $E^1_{red}$ was 0.196 V, whereas the measured value is −0.093 V[44]). Clearly, correlation analysis using the full Marcus−Eberson model and $\Delta G^{\circ\prime}$ from independently determined data is a more robust method for diagnosing the consistency of kinetic data with electron transfer theory.

For the practical objective of developing a QSAR for predicting reduction rates of energetic NACs, however, the above discussion of results in Figure 2, taken together with the prior evidence regarding rate limitation in these reactions,[11−15] suggests that (L)FER with a mechanistic basis in electron transfer theory (for the first electron transfer) are not broadly applicable to the variety of reductants of interest. However, simple linear correlations to $E^1_{NAC}$ are common and generally quite good, so they should be adequate for predicting rate constants. Such empirical correlations may arise because of covariation between $E^1_{NAC}$ and the factors influencing nitro reduction rates, but this is not problematic as long as the covariation holds. To avoid implying a specific mechanistic basis for the simple linear correlations to $E^1_{NAC}$, however, we discontinue the normalization of the slope to 0.059 V (cf. eq 1) and switch from using "LFER" to more general term "QSAR" to describe this correlation.[20]

In addition to selecting a simple linear correlation to $E^1_{NAC}$ as most appropriate model for developing a QSAR, we chose to focus on one reductant, Fe(II)P, as a model system for QSAR calibration. This choice was made to take advantage of the availability of existing data for nonenergetic model compounds and the simplicity of performing and analyzing experiments


DOI: 10.1021/es505092s
Environ. Sci. Technol. 2015, 49, 3778−3786

(especially compared to Fe(II)−tiron and Fe(II)−DFOB, where corrections for speciation are a major concern[41,42]).

**Calculated $E^1_{NAC}$ for QSAR Calibration.** To develop and validate QSARs for predicting reduction rates of energetic NACs, $E^1_{NAC}$ were calculated at several levels of theory, using the 6-311++G(2d,2p) basis set with the LDA, PBE, PBE0, B3LYP, and M06-2X exchange correlation functionals with solvation determined using the COSMO and/or COSMO-SMD solvation models. The results were evaluated by comparing a subset of the calculated $E^1_{NAC}$ values to a previously compiled set of measured $E^1_{NAC}$.[51] The validation data set is given in Table 1 along with the corresponding computed values determined at the levels of theory used in this study. The deviations between calculated and measured values were determined and are summarized (at the bottom of Table 1) as the mean absolute deviation (MAD), root-mean-square deviation (RMSD), and the largest positive and negative deviation.

The lowest MAD given in Table 1 corresponds with the data set obtained with the M06-2X exchange correlation functional and COSMO solvation model. This data set also gives the second lowest RMSD (0.001 V higher than the data set determined with the same exchange correlation functional and the COSMO-SMD solvation model). Comparing this computational method to previous efforts to determine $E^1_{NAC}$,[23−26,28] the M06-2X/COSMO method used here is the most accurate method currently reported for directly calculating $E^1_{NAC}$, and nearly as accurate as a method where $E^1_{NAC}$ is determined via correlation to calculated values of the adiabatic electron affinity[51] (MAD = 0.024 V, RMSD = 0.001 V, largest positive deviation = 0.071 V, largest negative deviation = −0.055 V).

To calibrate a QSAR using the $E^1_{NAC}$ values calculated using the M06-2X/COSMO method ($E^1_{NAC,\ M06\text{-}2X/COSMO}$), previously reported values of $k_{Fe(II)P}$ (also shown in Figure 2A and B) were correlated against $E^1_{NAC,\ M06\text{-}2X/COSMO}$ and fit by linear regression (Figure 3). A data point for chloronitrobenzene (3-Cl-NB) was treated as an outlier and excluded from the fit due to its anomalously large average deviation in $E^1_{NAC,\ M06\text{-}2X/COSMO}$ (3-Cl-NB is the only compound in Figure 3 for which the absolute deviation between $E^1_{NAC,\ M06\text{-}2X/COSMO}$ and the measured $E^1_{NAC}$ is larger than the MAD (0.166 vs 0.066 V)). The $r^2$ value for the resulting correlation is 0.74. Because the $r^2$ value for a similar correlation to measured values of $E^1_{NAC}$ (not shown) is 0.93, it can be concluded that much of the scatter of the data about the fit is related to error in $E^1_{NAC,\ M06\text{-}2X/COSMO}$. The QSAR resulting from the fit of the data is given in eq 7 (with standard deviations of the fitting coefficients in parentheses).

$$\log(k_{Fe(II)P}) = 7.6(\pm 1.7)\cdot E^1_{NAC,M06\text{-}2X/COSMO} + 4.07(\pm 0.82) \quad (7)$$

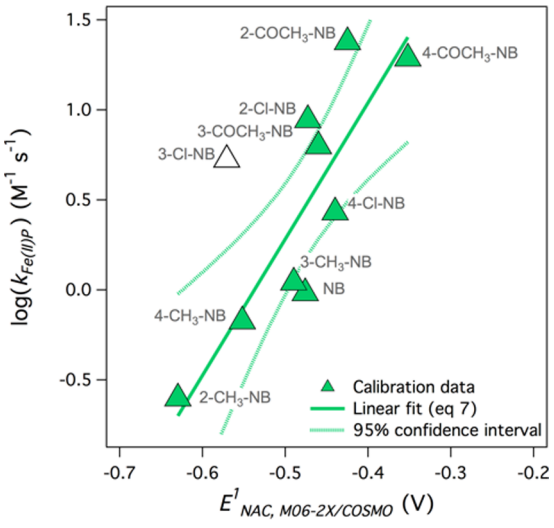


**Figure 3.** QSAR for NAC reduction by Fe(II)P calibrated using rate constants ($\log(k_{Fe(II)P})$) obtained from the literature[8] and $E^1_{NAC}$ calculated at the M06-2X/6-311++G(2d,2p) level with the COSMO solvation model (denoted as $E^1_{NAC,\ M06\text{-}2X/COSMO}$). The data point for 3-Cl-NB was treated as an outlier. The 95% confidence interval for the linear fit is also shown.

**Validation of the QSAR for Energetic NACs.** To validate the QSAR given in eq 7 for predicting rate constants for energetic compounds, we measured rate constants for reduction of three energetic NACs (TNT, 2,4-DNT, and DNAN) by Fe(II)P/cysteine. Rate constants were also measured for three nonenergetic NACs (NB, 4-Cl-NB, and 1,3-DNB) in order to check the agreement between our results and the previously published $k_{Fe(II)P}$ data we used to calibrate the FER given in eq 7.

A typical analysis of the measured kinetic data is shown in Figure 4 for 2,4-DNT. Data for the other compounds can be found in the SI, Table S8. Concentration vs time data for NAC disappearance at different Fe(II)P concentrations were fit to pseudo-first-order kinetics[8,9] to obtain observed rate constants ($k_{obs}$). These $k_{obs}$ were plotted against [Fe(II)P] and fit to a line to obtain the second-order rate constant $k_{Fe(II)P}$. Data for NB, 4-Cl-NB, and 2,4-DNT were fit in this manner. For some of the NACs tested, the concentration vs time plots showed progressive increases in rate that are not captured by the first-order model. This effect was especially pronounced for DNAN (Figure 5), but was also evident in concentration vs time plots for 1,3-DNB and TNT (SI, Table S8). These deviations from first-order kinetics are likely the result of

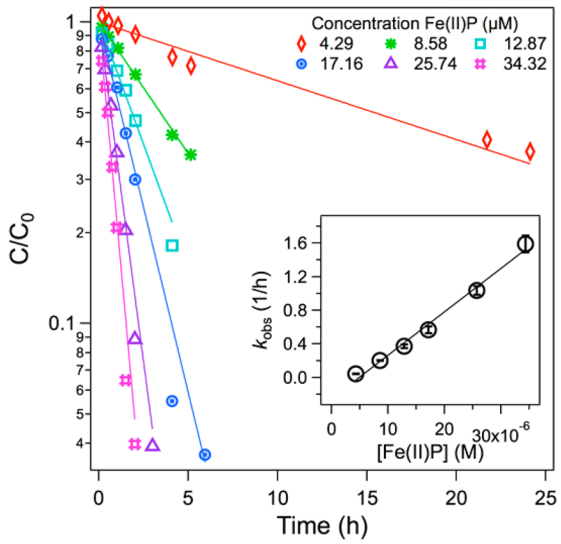


**Figure 4.** Concentration vs time plots of 2,4-DNT disappearance at various [Fe(II)P] with pseudo-first-order fits. Inset: $k_{obs}$ from the pseudo-first order fits vs nominal [Fe(II)P] with linear fit.



DOI: 10.1021/es505092s
Environ. Sci. Technol. 2015, 49, 3778−3786

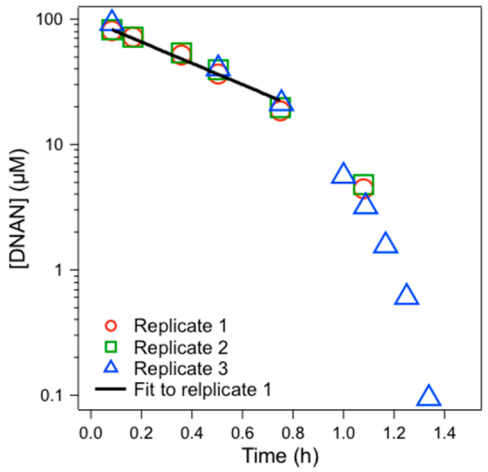


**Figure 5.** DNAN disappearance at 34.32 $\mu$M Fe(II)P with an initial portion of the data fit to pseudo-first-order kinetics.

secondary reactions (e.g., condensations involving intermediates), but this was not investigated further.

In the absence of a comprehensive kinetic model for the cases that show deviation from first-order behavior, the initial portion of the data alone were fit to first-order kinetics (similar to the method of initial rates[52]). This treatment resulted in fitting one to three half-lives of NAC disappearance data. It is likely that the kinetics at the beginning of the experiment were dominated by simple reduction of the nitro groups, making this simplification a satisfactory approximation of the rate constant for that process. Details regarding data fitting for all the NACs evaluated are given in the SI, Section 4. The resulting $\log(k_{Fe(II)P})$ values are reported in Table 2.

**Table 2. QSAR Verification and Validation Data**[a]

| NAC | $k_{Fe(II)P}$ (L $M^{-1}$ $s^{-1}$) | $\log(k_{FeP})$ |
|---|---|---|
| NB | 1.06 ± 0.16 | 0.026 |
| 4-Cl-NB | 1.946 ± 0.083 | 0.289 |
| 1,3-DNB | 16.6 ± 0.77 | 1.22 |
| 2,4-DNT | 14.34 ± 0.76 | 1.156 |
| TNT | 112.1 ± 3.1 | 2.050 |
| DNAN | 17.50 ± 0.55 | 1.243 |

[a] $k_{Fe(II)P}$ were determined from experimental data presented in the SI, Table S8.

To verify that our methods of measuring $k_{Fe(II)P}$ produced values similar to the calibration data set, $\log(k_{Fe(II)P})$ values for a few nonenergetic compounds (NB, 4-Cl-NB, and 1,3-DNB) were measured and plotted with the calibration data from Figure 3, as shown in Figure 6. The data for compounds in both the calibration and validation data sets (NB and 4-Cl-NB) show good agreement (deviations of <0.15 log units) between each pair of values and with the QSAR overall (deviations of <0.5 log units). An additional compound not found in the calibration data set, 1,3-DNB shows good agreement with the $k_{Fe(II)P}$ predicted by the QSAR (deviation of 0.07 log units). Overall, these results support the consistency of all three types of data (measured in previous work, measured in this work, and calculated from the QSAR). In addition, the results suggest that the measured values of $k_{Fe(II)P}$ are generally accurate and that most of the scatter observed in Figure 6 comes from $E^1_{NAC,\ M06\text{-}2X/COSMO}$ or limitations of the QSAR.

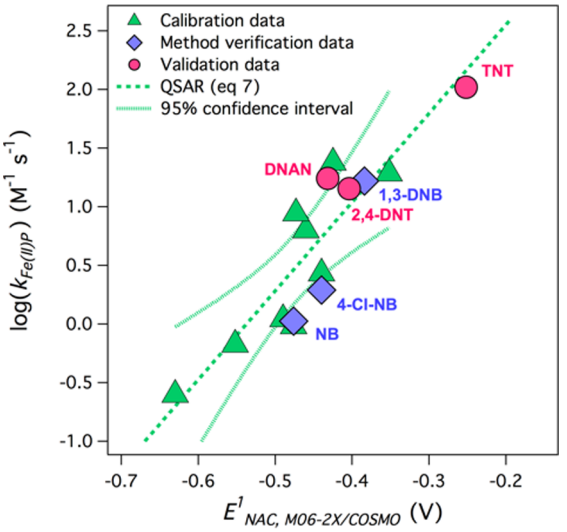


**Figure 6.** Comparison of newly collected $\log(k_{Fe(II)P})$ data to the calibration data set and QSAR. Data for nonenergetic NACs were used to verify agreement of the new data with the calibration data (method verification data). Data for energetic NACs were used to test the validity of the QSAR to energetic compounds (validation data).

Following method verification, $\log(k_{Fe(II)P})$ data for the energetic compounds tested (2,4-DNT, TNT, and DNAN) were appended to Figure 6 to test the validity of the QSAR to energetic compounds. The data points for TNT and 2,4-DNT plot nearly in line with the QSAR (with deviations of −0.105 and 0.156 log units, respectively) and are well within the 95% confidence interval for the QSAR (or extrapolation of this interval). The data point for DNAN falls just outside the 95% confidence interval, but within the range of scatter in the calibration data (with a deviation of 0.457 log units). The general agreement of the energetic NAC data with the QSAR suggests that this model may be used for estimating reduction rates by Fe(II)P. This information could be valuable in (i) making qualitative assessments of relative reduction rate constants for energetic NACs and (ii) guiding future experimentation (where more accurate data can be obtained for particular compounds and conditions).

## ■ ASSOCIATED CONTENT

### Supporting Information

Data and calculation details for Figure 2, detailed computational methods, comparisons of calculated and measured $E^1_{NAC}$ values, and detailed NAC disappearance data. This material is available free of charge via the Internet at http://pubs.acs.org.

## ■ AUTHOR INFORMATION

### Corresponding Author

*E-mail: tratnyek@ohsu.edu; phone: 503-346-3431; fax: 503-346-3427.

### Notes

The authors declare no competing financial interest.

## ■ ACKNOWLEDGMENTS

This work was supported by the Strategic Environmental Research and Development Program (SERDP) under ER-1735. This report has not been subject to review by SERDP and therefore does not necessarily reflect their views and no official endorsement should be inferred. A. J. S.-B. was supported as an



DOI: 10.1021/es505092s
Environ. Sci. Technol. 2015, 49, 3778−3786

OHSU Graduate Research Scholar during a portion of this study. A portion of this research was performed using the PNNL Institutional Computing (PIC) facility and the Chinook, Spokane, Barracuda, and Cascade computing resources at the Molecular Science Computing Facility at EMSL, a national scientific user facility sponsored by the Department of Energy's Office of Biological and Environmental Research located at Pacific Northwest National Laboratory, DE-AC06-76RLO 1830. We also acknowledge EMSL for supporting the development of NWChem. The Pacific Northwest National Laboratory is operated by Battelle Memorial Institute. Structure database management and sorting was performed using Instant JChem (Instant JChem 5.9.4, 2012, ChemAxon (http://www.chemaxon.com)).

## REFERENCES

(1) Talmage, S. S.; Opresko, D. M.; Maxwell, C. J.; Welsh, C. J. E.; Cretella, F. M.; Reno, P. H.; Daniel, F. B. Nitroaromatic munition compounds: Environmental effects and screening values. *Rev. Environ. Contam. Toxicol.* **1999**, *161*, 1−156.

(2) Juhasz, A. L.; Naidu, R. Explosives: Fate, dynamics, and ecological impact in terrestrial and marine environments. *Rev. Environ. Contam. Toxicol.* **2007**, *191*, 163−215.

(3) ASTM Standard E 2552. *Standard Guide for Assessing the Environmental and Human Health Impacts of New Energetic Compounds*; ASTM International: West Conshohocken, PA, 2008.

(4) Anastas, P. T.; Warner, J. C. *Green Chemistry: Theory and Practice*; Oxford University Press: Oxford, 1998.

(5) Salter-Blanc, A. J.; Bylaska, E. J.; Ritchie, J.; Tratnyek, P. G. Mechanisms and kinetics of alkaline hydrolysis of the energetic nitroaromatic compounds 2,4,6-trinitrotoluene (TNT) and 2,4-Dinitroanisole (DNAN). *Environ. Sci. Technol.* **2013**, *47*, 6790−6798.

(6) Schwarzenbach, R. P.; Gschwend, P. M.; Imboden, D. M. *Environmental Organic Chemistry*, 2nd ed.; Wiley: Hoboken, NJ, 2003.

(7) Larson, R. A.; Weber, E. J. Chapter 3. Reduction. In *Reaction Mechanisms in Environmental Organic Chemistry*; Lewis: Chelsea, MI, 1994; pp 169−215.

(8) Schwarzenbach, R. P.; Stierli, R.; Lanz, K.; Zeyer, J. Quinone and iron porphyrin mediated reduction of nitroaromatic compounds in homogeneous aqueous solution. *Environ. Sci. Technol.* **1990**, *24*, 1566−1574.

(9) Hofstetter, T. B.; Heijman, C. G.; Haderlein, S. B.; Holliger, C.; Schwarzenbach, R. P. Complete reduction of TNT and other (poly)nitroaromatic compounds under iron-reducing subsurface conditions. *Environ. Sci. Technol.* **1999**, *33*, 1479−1487.

(10) Tratnyek, P. G.; Weber, E. J.; Schwarzenbach, R. P. Quantitative structure-activity relationships for chemical reductions of organic contaminants. *Environ. Toxicol. Chem.* **2003**, *22*, 1733−1742.

(11) Laviron, E.; Meunier-Prest, R.; Vallat, A.; Roullier, L.; Lacasse, R. The reduction mechanism of aromatic nitro compounds in aqueous medium. Part II. The reduction of 4-nitropyridine between H0 = −6 and pH 9.6. *J. Electroanal. Chem.* **1992**, *341*, 227−255.

(12) Laviron, E.; Roullier, L. The reduction mechanism of aromatic nitro compounds in aqueous medium. Part I. Reduction to dihydroxylamines between pH 0 and 5. *J. Electroanal. Chem.* **1990**, *288*, 165−175.

(13) Hartenbach, A.; Hofstetter, T. B.; Berg, M.; Bolotin, J.; Schwarzenbach, R. P. Using nitrogen isotope fractionation to assess abiotic reduction of nitroaromatic compounds. *Environ. Sci. Technol.* **2006**, *40*, 7710−7716.

(14) Hartenbach, A. E.; Hofstetter, T. B.; Aeschbacher, M.; Sander, M.; Kim, D.; Strathmann, T. J.; Arnold, W. A.; Cramer, C. J.; Schwarzenbach, R. P. Variability of nitrogen isotope fractionation during the reduction of nitroaromatic compounds with dissolved reductants. *Environ. Sci. Technol.* **2008**, *42*, 8352−8359.

(15) Hofstetter, T. B.; Neumann, A.; Arnold, W. A.; Hartenbach, A. E.; Bolotin, J.; Cramer, C. J.; Schwarzenbach, R. P. Substituent effects on nitrogen isotope fractionation during abiotic reduction of nitroaromatic compounds. *Environ. Sci. Technol.* **2008**, *42*, 1997−2003.

(16) Marcus, R. A. Chemical and electrochemical electron-transfer theory. *Annu. Rev. Phys. Chem.* **1964**, *15*, 155−196.

(17) Eberson, L. *Electron Transfer Reactions in Organic Chemistry*; Springer-Verlag: Berlin, 1987.

(18) Meisel, D. Free energy correlation of rate constants for electron transfer between organic systems in aqueous solutions. *Chem. Phys. Lett.* **1975**, *34*, 263−266.

(19) Tratnyek, P. G.; Hoigné, J. Kinetics of reactions of chlorine dioxide (OClO) in water. II. Quantitative structure-activity relationships for phenolic compounds. *Water Res.* **1994**, *28*, 57−66.

(20) Tratnyek, P. G. Correlation analysis of the environmental reactivity of organic substances. In *Perspectives in Environmental Chemistry*; Macalady, D. L., Ed.; Oxford: New York, 1998; pp 167−194.

(21) Canonica, S.; Tratnyek Paul, G. Quantitative structure-activity relationships for oxidation reactions of organic chemicals in water. *Environ. Toxicol. Chem.* **2003**, *22*, 1743−1754.

(22) Ferry, J. L.; Glaze, W. H. Photocatalytic reduction of nitroorganics over illuminated titanium dioxide: Electron transfer between excited-state $TiO_2$ and nitroaromatics. *J. Phys. Chem. B* **1998**, *102*, 2239−2244.

(23) Zubatyuk, R. I.; Gorb, L.; Shishkin, O. V.; Qasim, M.; Leszczynski, J. Exploration of density functional methods for one-electron reduction potential of nitrobenzenes. *J. Comput. Chem.* **2010**, *31*, 144−150.

(24) Phillips, K. L.; Chiu, P. C.; Sandler, S. I. Reduction rate constants for nitroaromatic compounds estimated from adiabatic electron affinities. *Environ. Sci. Technol.* **2010**, *44*, 7431−7436.

(25) Uchimiya, M.; Gorb, L.; Isayev, O.; Qasim, M. M.; Leszczynski, J. One-electron standard reduction potentials of nitroaromatic and cyclic nitramine explosives. *Environ. Pollut. (Oxford, U. K.)* **2010**, *158*, 3048−3053.

(26) Bylaska, E. J.; Salter-Blanc, A. J.; Tratnyek, P. G. One-electron reduction potentials from chemical structure theory calculations. In *Aquatic Redox Chemistry*; Tratnyek, P. G., Grundl, T. J., Haderlein, S. B., Eds.; American Chemical Society: Washington, DC, 2011; ACS Symposium Series, Vol. *1071*; pp 37−64.

(27) Marenich, A. V.; Ho, J.; Coote, M. L.; Cramer, C. J.; Truhlar, D. G. Computational electrochemistry: Prediction of liquid-phase reduction potentials. *Phys. Chem. Chem. Phys.* **2014**, *16*, 15068−15106.

(28) Sviatenko, L.; Isayev, O.; Gorb, L.; Hill, F.; Leszczynski, J. Toward robust computational electrochemical predicting the environmental fate of organic pollutants. *J. Comput. Chem.* **2011**, *32*, 2195−2203.

(29) Scandola, F.; Balzani, V.; Schuster, G. B. Free-energy relationships for reversible and irreversible electron-transfer processes. *J. Am. Chem. Soc.* **1981**, *103*, 2519−2523.

(30) Klamt, A.; Schüürmann, G. COSMO: A new approach to dielectric screening in solvents with explicit expressions for the screening energy and its gradient. *J. Chem. Soc., Perkin Trans. 2* **1993**, 799−803.

(31) Valiev, M.; Bylaska, E. J.; Govind, N.; Kowalski, K.; Straatsma, T. P.; Van Dam, H. J. J.; Wang, D.; Nieplocha, J.; Apra, E.; Windus, T. L.; de Jong, W. A. NWChem: A comprehensive and scalable open-source solution for large scale molecular simulations. *Comput. Phys. Commun.* **2010**, *181*, 1477−1489.

(32) Kohn, W.; Sham, L. J. Self-consistent equations including exchange and correlation effects. *Phys. Rev. B* **1965**, *A140*, 1133−1138.

(33) Clark, T.; Chandrasekhar, J.; Spitznagel, G. W.; Schleyer, P. v. R. Efficient diffuse function-augmented basis sets for anion calculations. III. The 3-21+G basis set for first-row elements, lithium to fluorine. *J. Comput. Chem.* **1983**, *4*, 294−301.

(34) Krishnan, R.; Binkley, J. S.; Seeger, R.; Pople, J. A. Self-consistent molecular orbital methods. XX. A basis set for correlated wave functions. *J. Chem. Phys.* **1980**, *72*, 650.



DOI: 10.1021/es505092s
*Environ. Sci. Technol.* 2015, 49, 3778−3786

(35) Vosko, S. H.; Wilk, L.; Nusair, M. Accurate spin-dependent electron liquid correlation energies for local spin density calculations: a critical analysis. *Can. J. Phys.* **1980**, *58*, 1200.
(36) Perdew, J. P.; Burke, K.; Ernzerhof, M. Generalized gradient approximation made simple. *Phys. Rev. Lett.* **1996**, *77*, 3865.
(37) Becke, A. D. Density-functional thermochemistry 3. The role of exact exchange. *J. Chem. Phys.* **1993**, *98*, 5648−5652.
(38) Lee, C.; Yang, W.; Parr, R. G. Development of the Colle-Salvetti correlation-energy formula into a functional of electron density. *Phys. Rev. B* **1988**, *37*, 785−789.
(39) Adamo, C.; Barone, V. Toward reliable density functional methods without adjustable parameters: The PBE0 model. *J. Chem. Phys.* **1999**, *110*, 6158.
(40) Zhao, Y.; Truhlar, D. G. The M06 suite of density functionals for main group thermochemistry, thermochemical kinetics, noncovalent interactions, excited states, and transition elements: Two new functionals and systematic testing of four M06-class functionals and 12 other functionals. *Theor. Chem. Acc.* **2008**, *120*, 215−241.
(41) Naka, D.; Kim, D.; Strathmann, T. J. Abiotic reduction of nitroaromatic compounds by aqueous iron(II)-catechol complexes. *Environ. Sci. Technol.* **2006**, *40*, 3006−3012.
(42) Kim, D.; Duckworth, O. W.; Strathmann, T. J. Hydroxamate siderophore-promoted reactions between iron(II) and nitroaromatic groundwater contaminants. *Geochim. Cosmochim. Acta* **2009**, *73*, 1297−1311.
(43) Lund, T.; Lund, H. Single electron transfer as rate-determining step in an aliphatic nucleophilic substitution. *Acta Chem. Scand.* **1986**, *40B*, 470−485.
(44) Mukherjee, T. One-electron reduction of juglone (5-hydroxy-1,4-naphthoquinone): A pulse radiolysis study. *Radiat. Phys. Chem.* **1987**, *29*, 455−462.
(45) Ölinger, K.; Buffington, G. D.; Ernster, L.; Cadenas, E. Effects of superoxide dismutase on the automation of substituted hydro- and semi-naphthoquinones. *Chem.-Biol. Interact.* **1990**, *73*, 53−76.
(46) Batchelor-McAuley, C.; Li, Q.; Dapin, S. M.; Compton, R. G. Volumetric characterization of DNA intercalators across the full pH range: Anthraquinone-2,6-disulfonate and anthraquinone-2-sulfonate. *J. Phys. Chem. B* **2010**, *114*, 4094.
(47) Strathmann, T. J. Redox reactivity of organically complexed iron(II) species with aquatic contaminants. In *Aquatic Redox Chemistry*; Tratnyek, P. G., Grundl, T. J., Haderlein, S. B., Eds.; American Chemical Society: Washington, DC, 2011; ACS Symposium Series, Vol. *1071*; pp 283−313.
(48) Evans, M. G.; Polanyi, M. Further considerations on the thermodynamics of chemical equilibria and reaction rates. *Trans. Faraday Soc.* **1936**, *32*, 1333−1360.
(49) Evans, M. G.; Polanyi, M. Inertia and driving force of chemical reactions. *Trans. Faraday Soc.* **1938**, *34*, 11−24.
(50) Eberson, L. Electron-transfer reactions in organic chemistry. *Adv. Phys. Org. Chem.* **1982**, *18*, 79−185.
(51) Phillips, K. L.; Sandler, S. I.; Chiu, P. C. A method to calculate the one-electron reduction potentials for nitroaromatic compounds based on gas-phase quantum mechanics. *J. Comput. Chem.* **2011**, *32*, 226−239.
(52) Brezonik, P. L. *Chemical Kinetics and Process Dynamics in Aquatic Systems*; Lewis: Boca Raton, FL, 1994.


DOI: 10.1021/es505092s
*Environ. Sci. Technol.* 2015, 49, 3778−3786